

Evaluation of the Virtual Crystal Approximation for Predicting Thermal Conductivity

Jason M. Larkin¹ and A. J. H. McGaughey^{2,*}

¹*Department of Mechanical Engineering
Carnegie Mellon University
Pittsburgh, PA 15213*

²*Department of Mechanical Engineering
Carnegie Mellon University
Pittsburgh, PA 15213*

(Dated: November 1, 2012)

Accurately predicting the thermal conductivity of a dielectric or semiconducting material requires the properties of phonons from the entire Brillouin zone. Accurate predictions of phonon properties for bulk systems can be made with anharmonic lattice dynamics theory using ab initio calculations. However, computational costs limit the size of unit cells in ab initio calculations to be less than 100 atoms, making it difficult to directly incorporate the effects of disorder. Alternatively, theory that treats disorder as a harmonic perturbation can be used to estimate the reduction in phonon lifetimes due to disorder scattering without the use of a large unit cell. Under this approximation, the disordered crystal is replaced with a perfect virtual crystal with properties equivalent to an averaging over the disorder (e.g. mass or bond strength). In this work, the virtual crystal approximation for mass disorder is evaluated by examining two model alloy systems: Lennard-Jones argon and Stillinger-Weber silicon. In both cases the perfect crystal is alloyed with a heavier mass species up to equal concentration. These two alloyed systems have different ranges of phonon frequencies, lifetimes, and mean free paths. For Stillinger-Weber silicon, the virtual crystal approximation predicts phonon properties and thermal conductivity in good agreement with molecular dynamics-based methods. For Lennard-Jones argon, the virtual crystal approximation underpredicts the high frequency phonon lifetimes, leading to an underpredicting of its thermal conductivity.

I. INTRODUCTION

For thermoelectric device applications, minimizing a thermoelectric material's thermal conductivity has become a promising technique for increasing $ZT > 3$.^{1,2} In semiconductor alloys, understanding the effect of disorder is necessary for optimizing ZT by further lowering thermal conductivity.³⁻⁶

Abeles first introduced the idea of using a virtual crystal (VC) to replace a disordered one by treating both disorder and anharmonicity as perturbations.⁸ Recently, work using ab-initio calculations and the virtual crystal approximation^{6,7}.

The goal of this work is to verify the use of the virtual crystal approximation for predicting thermal conductivity by a detailed comparison of 3 methods for predicting thermal conductivity: MD-based normal mode decomposition (NMD) and green-kubo (GK), and anharmonic lattice dynamics (ALD) which treats the harmonic and anharmonic phonon scattering as perturbations. Two model alloy systems with mass defects are considered: Lennard-Jones argon and Stillinger-Weber silicon. In both cases the perfect crystal is alloyed with a heavier mass species up to equal concentration. These two alloyed systems have different ranges of phonon frequencies, lifetimes, and mean free paths. For Stillinger-Weber silicon, ALD predicts phonon properties and thermal conductivity in good agreement with MD-based methods NMD and GK. For Lennard-Jones argon, the VC approximation underpredicts the high frequency phonon lifetimes, leading to an underpredicting of its thermal

conductivity.

II. VIRTUAL CRYSTAL (VC) APPROXIMATION

Abeles introduced the idea of using a virtual (perfect) crystal to replace a disordered one, computing the thermal conductivity of Si/Ge alloys by treating both disorder and anharmonicity as perturbations.⁸ Cahill shows that conductivity of dilute Ge-doped Si epitaxial layers agrees with a virtual crystal approximation and defect scaling (see section).¹⁸ Garg showed using ab initio calculations that the virtual crystal approximation works well for Si-Ge for all concentrations.⁷ A detailed study of PbTe/PbSe systems demonstrate the importance of bond environment for alloys.⁶

The computaitonal studies discussed above were limited

We calculate at all compositions the phonon modes of the virtual crystal (which has a lattice parameter, mass, and force constants of that particular composition) and derive from those the frequencies, group velocities, and lifetimes to calculate thermal conductivity.

A. VC and Gamma DOS Comparison

Bouchard show that alloy DOS varies smoothly with concentration for a- Si_xGe_{1-x} .²⁰

The low frequency

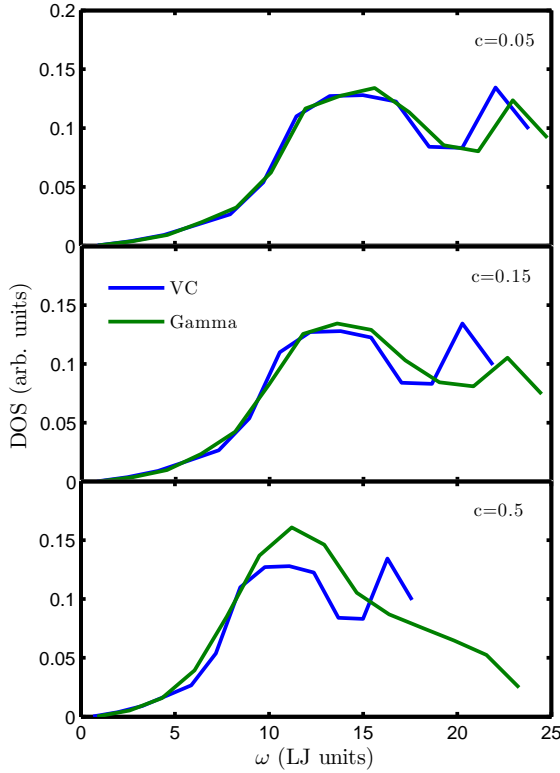


FIG. 1: virtual crystal results

B. Structure Factor of Gamma Point Modes

$$E^L(\kappa) = \left| \sum_{l,b} \hat{\kappa} \cdot e(\kappa_b^\alpha) \exp[i\kappa \cdot \mathbf{r}_0(b)] \right|^2 \quad (1)$$

$$E^T(\kappa) = \left| \sum_{l,b} \hat{\kappa} \times e(\kappa_b^\alpha) \exp[i\kappa \cdot \mathbf{r}_0(b)] \right|^2 \quad (2)$$

$$S^{L,T}(\omega) = \sum_\nu E^{L,T}(\kappa) \delta(\omega - \omega(\kappa)) \quad (3)$$

Demonstrates the importance of dispersion, even along different lattice directions ([100] vs [111]) and polarizations ($S^{L,T}$).

With increasing concentration, the structure factor spreads in width, particularly at high frequencies. The VC mass becomes larger and the peaks in the structure factor shift to lower frequencies.

III. KINETIC THEORY

For a perfect system, all vibrational modes are phonons.

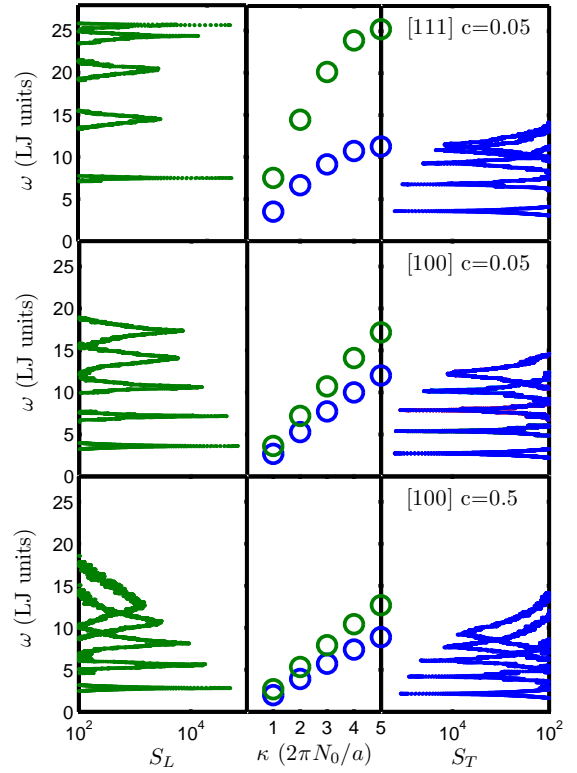


FIG. 2: virtual crystal results

Using the single-mode relaxation time approximation⁷ as an approximate solution of the Boltzmann transport equation⁷ gives

$$k_{vib,\mathbf{n}} = \sum_\kappa \sum_\nu c_{ph}(\kappa) \mathbf{v}_{g,\mathbf{n}}^2(\kappa) \tau(\kappa). \quad (4)$$

Here, c_{ph} is the phonon volumetric specific heat and $\mathbf{v}_{g,\mathbf{n}}$ is the component of the group velocity vector in direction \mathbf{n} . Since the systems we consider are classical and obey Maxwell-Boltzmann statistics,¹⁰ the specific heat is k_B/V per mode in the harmonic limit where V is the system volume. This approximation is used here and has been shown to be suitable for LJ argon¹¹ and SW silicon.¹²

A. Phonon Group Velocities

The group velocity vector is the gradient of the dispersion curves (i.e., $\partial\omega/\partial\kappa$), which can be calculated from the frequencies and wavevectors using finite differences. In this work, the group velocities are calculated using finite difference and quasi-harmonic lattice dynamics because a very small finite difference can be used which reduces the error.[?]

Of particular interest if the phonon mean free path (MFP),

$$\Lambda(\kappa) = |\mathbf{v}_g| \tau(\kappa), \quad (5)$$

which requires a group velocity.

In ordered systems, the group velocity generally scales with both the density and stiffness of the material. For example, the reduced vibrational conductivity of Ge compared to Si can be (partially) explained in both in terms of the \bar{m} (germanium has a larger density ρ than silicon) and the group velocity (germanium has a smaller bulk modulus B , and $v_g \propto \sqrt{B/\rho}$). Thus, for alloys, there should also be a corresponding scaling of the group velocity with the alloy's concentration (mass density). Duda shows the reduction in group velocity of disordered systems.²¹

B. Phonon Lifetimes

$$\frac{1}{\tau(\kappa)} = \frac{1}{\tau_{p-p}(\kappa)} + \frac{1}{\tau_d(\kappa)}, \quad (6)$$

where $\tau_{p-p}(\kappa)$ accounts for phonon-phonon scattering, accounts for boundary scattering, $\tau_d(\kappa)$ accounts for defect scattering.

Phonon-phonon scattering ($\tau_{p-p}(\kappa)$) is typically treated using anharmonic perturbation theory including only 3-phonon processes.^{6,7,13} It has been estimated that the effects of higher order phonon processes are small⁷. At low frequencies, $\tau_{p-p}(\kappa)$ follows a scaling due to both normal ($B_1\omega^2$) and umklapp ($B_2\omega^2$) 3-phonon scattering processes, where the density of states is Debye-like. The constants B_1 and B_2 are typically fit to experimental data.

Using harmonic perturbation theory, Tamura gives a general expression for mass point defect scattering¹⁶

$$\frac{1}{\tau_d(\kappa)} = \frac{\pi}{2N} \omega(\kappa)^2 \sum_{\kappa' \nu'} \delta(\omega(\kappa') - \omega(\kappa')) \sum_b g(b) |e^*(\kappa' \nu' \alpha) \cdot e(\kappa \nu \alpha)|^2, \quad (7)$$

where $g(b) = \sum_i c_i(b)(1 - m_i(b)/\bar{m}(b))^2$, N is the number of unit cells, and c_i is the fraction, m_i is the mass, and \bar{m}_i is the average mass of the i -th species.

At low frequencies, the phonon scattering due to mass point-defects is given by $A\omega^{-4}$, where A is a constant related to the unit cell volume, branch-averaged group velocity, and disorder coupling strength (g in Eq. above). The frequency dependence (ω^4) is the same as Rayleigh scattering, which is valid at low frequency where the Debye approximation is valid. Bond disorder can be accounted for using a similar expression with an average atomic radius or suitable scattering cross-section.^{14,15}

Cahill shows that conductivity reduction in dilute Ge-doped Si epitaxial layers is captured mostly by the mass disorder.¹⁸ The effect of bond and mass disorder has been investigated computationally by Skye and Schelling for Si/Ge¹⁹, where it was shown that mass disorder is the dominant scattering mechanism. In this work we consider only mass disorder.

While the expression for harmonic defect scattering (Eq.) is valid for perturbative disorder, its use leads to good agreement with several experimental and computational results with large disorder. , even in the case of the Ni0:55 Pd0:45 alloy, where the atomic species are chemically similar but mass disorder is large ($m_{\text{Pd}} = m_{\text{Ni}}$ 14:1812) [20].

6,7,13

Cahill shows that even though the mass difference between Si and Ge is larger than the mass of Si, the defect scaling agrees with experimental measurements of thermal conductivity in dilute SiGe epitaxial layers.¹⁷

IV. PHONON LIFETIME PREDICTIONS

A. Normal Mode Decomposition (NMD)

We use the normal mode decomposition (NMD) method

The phonon lifetime is predicted using the following

$$\tau(\kappa) = \int_0^\infty \frac{\langle E(\kappa; t) E(\kappa; 0) \rangle}{\langle E(\kappa; 0) E(\kappa; 0) \rangle} dt \quad (8)$$

The phonon normal mode coordinates, $q(\kappa; t)$ and $q(\kappa; 0)$, are required to calculate the phonon normal mode energy $E(\kappa)(t)$. The phonon mode eigenvectors, $e(\kappa \nu \alpha)$, are required to map the atomic coordinates onto the phonon normal modes. Under the VC approximation, the phonon eigenvectors are those of pure plane-waves. In a disordered supercell, the vibrational modes are not purely plane-wave (phonon) (see Section) and exist at the Gamma point ([000]). Both cases

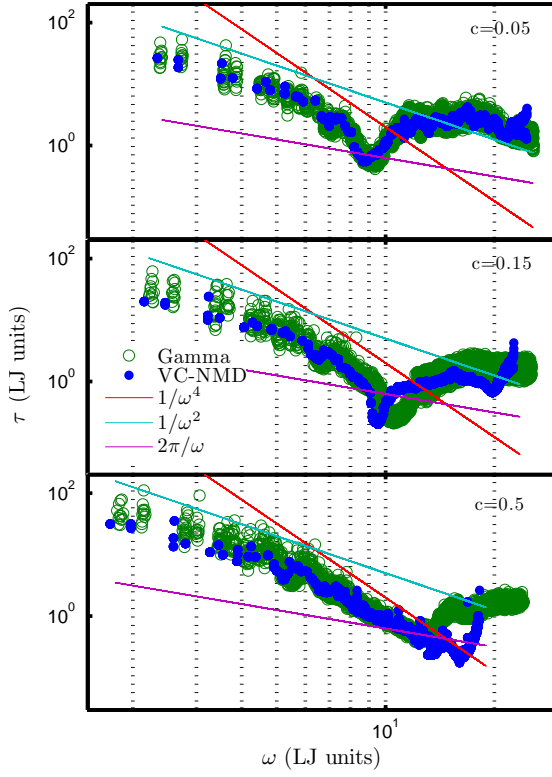


FIG. 3: virtual crystal results

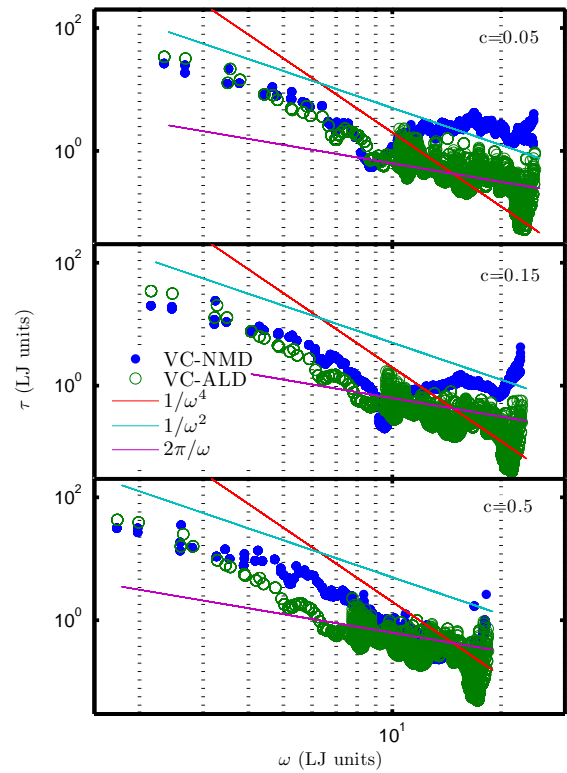


FIG. 4: gamma point results

B. NMD-VC and Gamma Point Phonon Lifetimes

C. NMD and ALD Lifetime Comparison

Essentially, the normal mode mappings are performed using eigenvectors which are plane waves.

V. THERMAL CONDUCTIVITY PREDICTIONS

An addition of as little as 10% Ge is sufficient to reduce the thermal conductivity to the minimum value achievable through alloying. Theoretically, mass disorder is found to increase the anharmonic scattering of phonons through a modification of their vibration eigenmodes. Notably, the thermal conductivity is found to drop sharply after only a small amount of alloying. This is due to the strong harmonic scattering of phonons even in the dilute alloy limit.

Duda shows that taking a perfect alloy and disordering via an order parameter allows control of thermal conductivity.²³

The thermal conductivity of amorphous solids at low temperatures contain quantum statistical effects.²² Molecular dynamics simulations are not able to capture quantum statistical effects.

VI. DISCUSSION

- compare lifetimes from 2 atom alloy, 4 atom alloy. Is the reduction in thermal conductivity mostly due to the reduction in group velocities/introduction of optical modes?

A. Boundary Scattering

Boundary scattering is responsible for decreasing the long lifetimes (mean free paths) of low frequency phonons

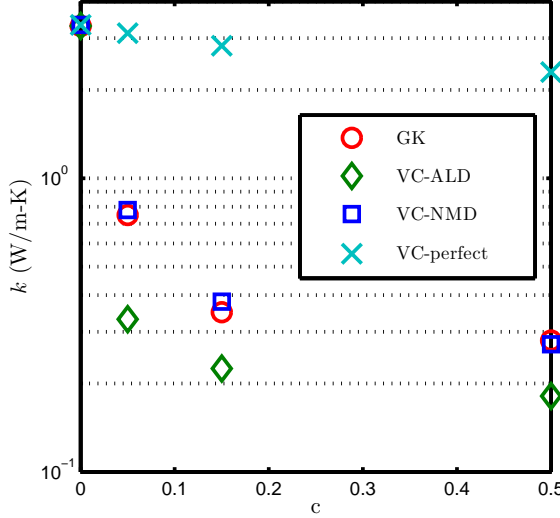


FIG. 5: The vibrational conductivity of LJ alloys predicted using MD simulations and the Green-Kubo method. The predicted thermal conductivities are for a LJ alloy of the form $m_{1-c}^a m_c^b$, where $m^a = 1$, $m^b = 3$, and $m_r = m^a/m^b = 3$ (in LJ units). As the alloy concentration is increased perturbatively, the vibrational conductivity drops quickly and saturates to a minimum at $c = 0.5$. For $c = 0.5$ the system is heavily disordered and the vibrational conductivity approaches that of an amorphous system.

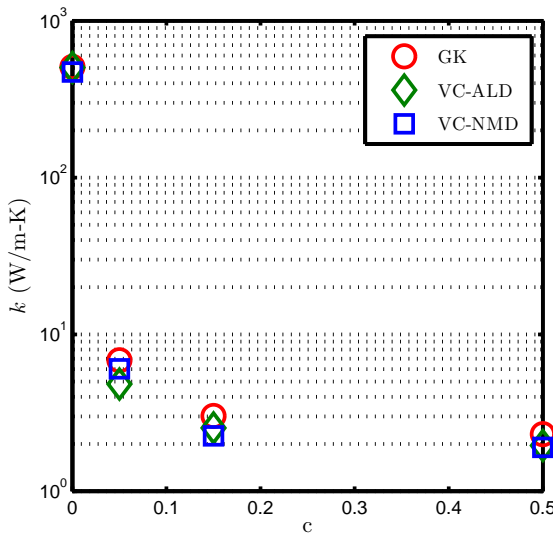


FIG. 6: The vibrational conductivity of LJ alloys predicted using MD simulations and the Green-Kubo method. The predicted thermal conductivities are for a LJ alloy of the form $m_{1-c}^a m_c^b$, where $m^a = 1$, $m^b = 3$, and $m_r = m^a/m^b = 3$ (in LJ units). As the alloy concentration is increased perturbatively, the vibrational conductivity drops quickly and saturates to a minimum at $c = 0.5$. For $c = 0.5$ the system is heavily disordered and the vibrational conductivity approaches that of an amorphous system.

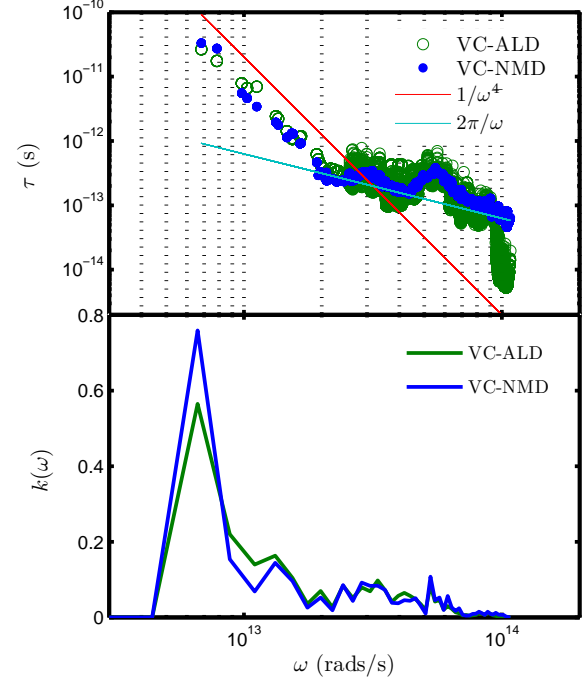


FIG. 7: gamma point results

which carry a significant amount of heat, making it particularly effective at decreasing the thermal conductivity of systems with length scale of 100s of nm and less.²⁴

First-principles calculations on some thermoelectric materials show that phonons have a wide MFP distribution, and hence relatively large nanostructures can reduce their lattice thermal conductivity.^{5,18,19} On the other hand, recent first-principles calculations have shown that the distribution is much narrower for PbTe,²⁰ and thus, further characterizations of the distributions and the associated detailed heat conduction of lead chalcogenides are important for better material design.

VII. SUMMARY

Appendix A: Allowed Wavevectors in Ordered and Disordered Systems

The phonon spectral energy is defined for the allowed wavevectors of a crystal, which can be specified from the crystal structure's Bravais lattice and its basis, i.e. unit cell. A D -dimensional Bravais lattice is a collection of points with positions

$$\mathbf{u}_0(l) = \sum_{\alpha}^D N_{\alpha} \mathbf{a}_{\alpha} \quad (A1)$$

where N_{α} and the summations if over the lattice vectors, \mathbf{a}_{α} .? The basis (or unit cell) is the building block of the crystal and they are arranged on the points defined by the

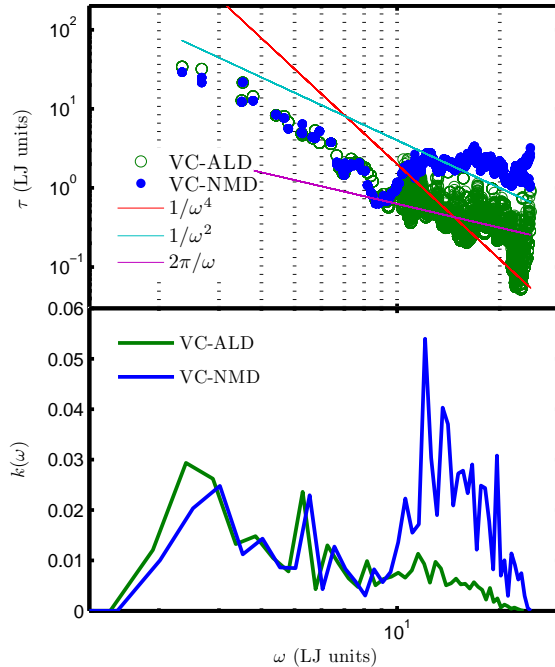


FIG. 8: gamma point results

Bravais lattice. The equilibrium position of any atom in the crystal can be described by

$$\mathbf{u}_0(l_b) = \mathbf{u}_0(l_0) + \mathbf{u}_0(b^0) \quad (\text{A2})$$

where $\mathbf{u}_0(l)$ is the equilibrium position of the l^{th} unit cell and $\mathbf{u}_0(b^0)$ is the equilibrium position of the b^{th} atom in the unit cell relative to $\mathbf{u}_0(l_0)$. For the LJ systems studied here, the cubic conventional cells are used with four atoms per unit cell.⁷ For our MD simulations, cubic simulation domains with periodic boundary conditions are used with $N_1 = N_2 = N_3 = N_0$.^{7, 8} The allowed wavevectors for such crystal structures are

$$\boldsymbol{\kappa} = \sum_{\alpha} \mathbf{b}_{\alpha} \frac{n_{\alpha}}{N_{\alpha}}, \quad (\text{A3})$$

where \mathbf{b}_{α} are the reciprocal lattice vectors⁷ and $-N_{\alpha}/2 < n_{\alpha} \leq N_{\alpha}/2$, where n_{α} are integers and N_{α} are even integers.⁷ The wavevectors are taken to be in the first Brillouin zone.⁷

Strictly speaking, the only allowed wavevector in a disordered system is the gamma point ($\boldsymbol{\kappa} = [000]$). As such, the lattice dynamics calculations are performed at the gamma point:

1. Normal Mode Decomposition

If $\gamma(\boldsymbol{\kappa}) > \omega(\boldsymbol{\kappa})$, then the vibrational mode is over-damped. Discuss why real-space method is necessary in this case.

Appendix B: Finite Simulation-Size Scaling for Thermal Conductivity

For the LJ argon system studied in Section ??, a finite simulation-size scaling procedure^{7, 8} is used to compare the thermal conductivity predictions from Φ and Φ' to those from the Green-Kubo method. The scaling procedure is demonstrated in Fig. ???. The thermal conductivity is predicted from Φ or Φ' and MD simulations with $N_0 = 4, 6, 8$, and 10. The bulk conductivity, k_{∞} , is then estimated by fitting the data to

$$1/k = 1/k_{\infty} + A/N_0, \quad (\text{B1})$$

where A is a constant. This procedure is necessary because the first Brillouin zone is only sampled at a finite number of points for a finite simulation size, with no contribution from the volume at its center. To predict a bulk thermal conductivity, it is important to sample points near the Brillouin zone center, where the modes can have large lifetimes and group velocities.^{7, 8}

-
- ^{*} Electronic address: mcgaughey@cmu.edu
- ¹ G. Chen, M. S. Dresselhaus, G. Dresselhaus, J.-P. Fleurial, and T. Caillat, International Materials Reviews **48**, 4566 (2003).
 - ² M. Dresselhaus, G. Chen, M. Tang, R. Yang, H. Lee, D. Wang, Z. Ren, J. Fleurial, and P. Gogna, Advanced Materials **19**, 10431053 (2007), ISSN 1521-4095, URL <http://dx.doi.org/10.1002/adma.200600527>.
 - ³ T. He, J. Chen, H. D. Rosenfeld, and M. A. Subramanian, Chemistry of Materials **18**, 759762 (2006).
 - ⁴ B. Huang and M. Kaviani, Acta Materialia **58**, 4516–4526 (2010), ISSN 1359-6454, URL <http://www.sciencedirect.com/science/article/pii/S1359645410002764>.
 - ⁵ E. S. Toberer, A. Zevalkink, and G. J. Snyder, J. Mater. Chem. **21** (2011), URL <http://dx.doi.org/10.1039/C1JM11754H>.
 - ⁶ Z. Tian, J. Garg, K. Esfarjani, T. Shiga, J. Shiomi, and G. Chen, Phys. Rev. B **85**, 184303 (2012), URL <http://link.aps.org/doi/10.1103/PhysRevB.85.184303>.
 - ⁷ J. Garg, N. Bonini, B. Kozinsky, and N. Marzari, Phys. Rev. Lett. **106**, 045901 (2011), URL <http://link.aps.org/doi/10.1103/PhysRevLett.106.045901>.
 - ⁸ B. Abeles, Phys. Rev. **131**, 19061911 (1963), URL <http://link.aps.org/doi/10.1103/PhysRev.131.1906>.
 - ⁹ P. B. Allen, J. L. Feldman, J. Fabian, and F. Wooten, Philosophical Magazine B **79**, 1715 (1999).
 - ¹⁰ D. A. McQuarrie, *Statistical Mechanics* (University Science Books, Sausalito, 2000).
 - ¹¹ A. J. H. McGaughey and M. Kaviani, Physical Review B **69**, 094303 (2004).
 - ¹² J. V. Goicochea, M. Madrid, and C. H. Amon, Journal of Heat Transfer **132**, 012401 (2010).
 - ¹³ J. E. Turney, PhD thesis, Carnegie Mellon University, Pittsburgh, PA (2009).
 - ¹⁴ P. G. Klemens, Proceedings of the Physical Society. Section A **68**, 1113 (1955), URL <http://stacks.iop.org/0370-1298/68/i=12/a=303>.
 - ¹⁵ P. G. Klemens, Proceedings of the Physical Society. Section A **70**, 833 (1957), URL <http://stacks.iop.org/0370-1298/70/i=11/a=407>.
 - ¹⁶ S.-i. Tamura, Phys. Rev. B **27**, 858866 (1983), URL <http://link.aps.org/doi/10.1103/PhysRevB.27.858>.
 - ¹⁷ D. G. Cahill, F. Watanabe, A. Rockett, and C. B. Vining, Phys. Rev. B **71**, 235202 (2005), URL <http://link.aps.org/doi/10.1103/PhysRevB.71.235202>.
 - ¹⁸ D. G. Cahill and F. Watanabe, Phys. Rev. B **70**, 235322 (2004), URL <http://link.aps.org/doi/10.1103/PhysRevB.70.235322>.
 - ¹⁹ A. Skye and P. K. Schelling, Journal of Applied Physics **103**, 113524 (2008), URL <http://link.aip.org/link/JAP/103/113524/1>.
 - ²⁰ A. M. Bouchard, R. Biswas, W. A. Kamitakahara, G. S. Grest, and C. M. Soukoulis, Phys. Rev. B **38**, 1049910506 (1988), URL <http://link.aps.org/doi/10.1103/PhysRevB.38.10499>.
 - ²¹ J. C. Duda, T. S. English, D. A. Jordan, P. M. Norris, and W. A. Soffa, Journal of Physics: Condensed Matter **23**, 205401 (2011), URL <http://stacks.iop.org/0953-8984/23/i=20/a=205401>.
 - ²² J. J. Freeman and A. C. Anderson, Physical Review B **34**, 5684\textbackslash (1986).
 - ²³ J. C. Duda, T. S. English, D. A. Jordan, P. M. Norris, and W. A. Soffa, Journal of Heat Transfer **134**, 014501 (2012).
 - ²⁴ A. J. H. McGaughey and A. Jain, Applied Physics Letters **100**, 061911 (2012), URL <http://link.aip.org/link/APL/100/061911/1>.
 - ²⁵ J. E. Turney, E. S. Landry, A. J. H. McGaughey, and C. H. Amon, Phys. Rev. B **79**, 064301 (2009), URL <http://link.aps.org/doi/10.1103/PhysRevB.79.064301>.